PHYSICAL REVIEW B **82**, 081306(R) (2010)

Spatio-temporal dynamics of coupled electrons and holes in nanosize CdSe-CdS semiconductor tetrapods

C. Mauser,[1] E. Da Como,[1,*] J. Baldauf,[1] A. L. Rogach,[1,†] J. Huang,[2] D. V. Talapin,[2] and J. Feldmann[1]
[1]*Photonics and Optoelectronics Group, Physics Department and CeNS, Ludwig-Maximilians-University, München, Germany*
[2]*Department of Chemistry, The University of Chicago, Chicago, Illinois 60637, USA*
(Received 16 July 2010; published 10 August 2010)

We report on coupled electron-hole transfer, Coulomb drag, in CdSe/CdS semiconductor nanotetrapods. We demonstrate that photoexcited holes can either be transferred to the CdSe core or become trapped in one of the CdS arms. By combining time-resolved pump-probe and photoluminescence measurements we investigate how the Coulomb potential drags the electron to the hole localization site. As supported by effective-mass calculations taking into account Coulomb effects we conclude that the hole dynamics determines the fate of the electron in a coupled dynamics.

DOI: 10.1103/PhysRevB.82.081306 PACS number(s): 78.67.Bf, 73.63.Nm, 78.47.J−, 78.55.−m

Coulomb interactions play a crucial role in determining the electronic and optical properties of semiconductors. Apart from being responsible for the formation of excitons, they can also influence carrier transport. Intriguing is the case of coupled transport, where electron and hole drift can be influenced by the Coulomb potential, Coulomb drag,[1,2] or ambipolar transport.[3] In semiconductors within the strong confinement regime, such as nanocrystal quantum dots, carriers are confined in space and thus expected to interact strongly due to the Coulomb potential.[4–6] While several phenomena such as exciton recombination or electron-hole separation depend on Coulomb interactions,[7,15] little is known on the effects on transport or relaxation. For *Coulomb drag* processes in coupled quantum wells, insulating barriers are used to avoid electron-hole recombination.[2] Indeed, when considering separated electrons and holes, recombination clearly limits the observation time for Coulomb mediated effects. Optical spectroscopy techniques, with femtosecond time resolution capable to access the early events after electron and hole generation, should give valuable information. Upon optical excitation with a femtosecond pulse hot electrons and holes are created, which subsequently relax according to the energy landscape. It remains a fundamental question how the Coulomb interaction controls the fate of the photogenerated charge carriers.

Most optical studies so far have been performed on spherical nanocrystals, where effects due to the strong spatial confinement and Coulomb interactions are difficult to distinguish.[7] Recently, heterostructured CdSe/CdS nanocrystals have been demonstrated to be interesting systems for applications.[8,9] Their peculiar band alignment results in valence subband levels at low energies localized in the CdSe and a conduction band where CdSe and CdS states are mixed, giving a delocalized electron wave function[10] [Fig. 1(a)]. Such an electronic structure represents a prototype for studying electron and hole Coulomb interactions, offering a landscape with energy gradients for the hole and a single band-edge state for the electron. We have chosen to study tetrapod-shaped nanoparticles,[11,12] where CdS rods are grown on top of a CdSe core with a tetrahedral geometry, further referred to as CdSe/CdS tetrapods. Their three-dimensional geometry is expected to enable isotropic Coulomb interactions and offers spatially separated energy sites for studying real-space dynamics optically. The energy landscape of CdSe/CdS favors hole localization in the CdSe or trapping to a defect in the CdS [cf. Fig. 1(a)] and can enable an electron wave function, which penetrates symmetrically in all arms.[12] A particularly interesting aspect of these nanocrystals is related to different states for the relaxed hole and a single conduction-band-edge state for the relaxed electron characterized by a delocalized wave function.

In this Rapid Communication, we report on the coupled dynamics of electrons and holes in CdSe/CdS tetrapods. The carrier dynamics is investigated by comparing femtosecond pump-probe and picosecond photoluminescence (PL) experiments. The combination of these techniques allows for monitoring of the dynamics of carriers populating the peripheral CdS arms or the central CdSe core. The experiments supported by model calculation demonstrate how the delocalized electron follows the hole dynamics as a consequence of the Coulomb interaction, providing evidence for coupled real-space dynamics in a semiconductor nanostructure.

Two samples have been studied, both with the CdSe core size of 4 nm and with variable CdS arm length: 16 nm for the S1 sample and 55 nm for the S2 sample (cf. Fig. 2). The tetrapods were dispersed in a transparent polymer drop-casted on quartz and placed in a cryostat at 5 K. Pump-probe spectroscopy was performed, exciting at 3.1 eV (400 nm) and probing the relative change in the transmission of a white light continuum (time resolution ~150 fs). The average number of excitons per particle was ~0.1 for both samples. A streak camera was used for PL experiments. Wave-function calculations were performed considering an effective Coulomb potential in a self-consistent iterative procedure as described in Refs. 12 and 13.

Figures 1(b)–1(d) show the electron and hole wave functions in a CdSe/CdS tetrapod for different configurations. The middle panel (c) illustrates the wave-function distributions, immediately after the excitation event at 3.1 eV. The hole is in the excited state which extends into the CdS and is delocalized over the overall tetrapod. From this state, it can still relax to the manifold of valence subband states confined within the CdSe core. The electron is shown in the lowest conduction subband and its density is centered in the tetra-

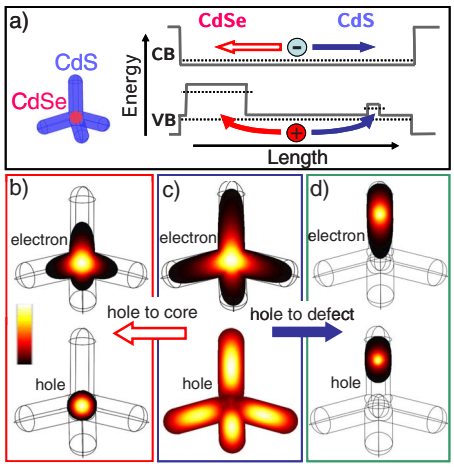

FIG. 1. (Color online) Calculated electron and hole wave functions in CdSe/CdS tetrapods in the presence of Coulomb interactions for different states of the hole. (a) Energy diagram plotted over a spatial coordinate going along the axis of one of the tetrapod arms. The arrows indicate the real-space dynamics of the electron and hole to the core (red arrow) or to a trapping site (blue arrow). (b) Electron and hole wave functions at the band edge of the structure with the hole confined in the CdSe. (c) Electron and hole at the band-edge states of CdS before relaxation of the hole to the CdSe core. (d) The hole wave function is localized in a low-energy trapping site in one of the CdS arms, resulting in the localization of the electron wave function to the same arm.

pod core. This configuration essentially describes the wave functions of carries in the states involved in the CdS band-edge transition. Holes can lose energy by localizing in the core as indicated by the red arrow in Fig. 1(a). Within the core, fast hole relaxation (subpicosecond) to the band edge occurs.[7,14] As a result of hole localization in the core, the electron wave function is slightly modified by experiencing a localized Coulomb potential in the core [Fig. 1(b)] while being still in the conduction-band-edge state. The energy of the Coulomb interaction is estimated to be ~75 meV.

In addition to the core localization described above, holes have a certain probability of being localized in the CdS arms [blue arrow in Fig. 1(a)]. In CdS, trap states are known to influence mostly the hole dynamics rather than the electron, as a consequence of the heavier hole mass.[15,16] The trap was accounted for in the simulations described below by introducing a shallow level in the valence band, where the hole wave function localizes. The electron wave function is perturbed by this configuration and localizes in the same arm as a consequence of Coulomb interaction [Fig. 1(d)]. Note that in this case the electron wave-function distribution was obtained solely by the Coulomb potential and does not require localization levels in the conduction band. It is the Coulomb potential that localizes in space the electron wave function toward the CdS. We have used the combination of pump-probe and PL experiments to find signatures of Coulomb interactions in the carrier dynamics. Figure 2(a) shows the differential transmission ($\Delta T/T$) as a function of the pump-probe delay time for the S1 sample at two different probe energies. In red we plot the signal probing the CdSe (1.9 eV) and in blue the CdS (2.7 eV) band-edge transitions. For direct comparison with $\Delta T/T$ data on S2, the CdS bleaching reported here has been normalized by the linear optical density at 2.7 eV, which is larger for S2 than for S1. As generally assumed for nanocrystals,[7,17] the $\Delta T/T$ signal is proportional to the state population, $\Delta T(\hbar\omega) \propto a_{\hbar\omega}[n_e(\hbar\omega)+n_h(\hbar\omega)]$ where a is the absorption cross section of the bleaching transition at a specific energy $\hbar\omega$ and n_e, n_h are the occupation numbers of the electron and hole states involved in the *bleached* transition. Here, we assume that electrons and holes have similar contributions to the bleaching. This is supported by the similar spacing between intraband levels in the conduction and valence band of CdSe/CdS

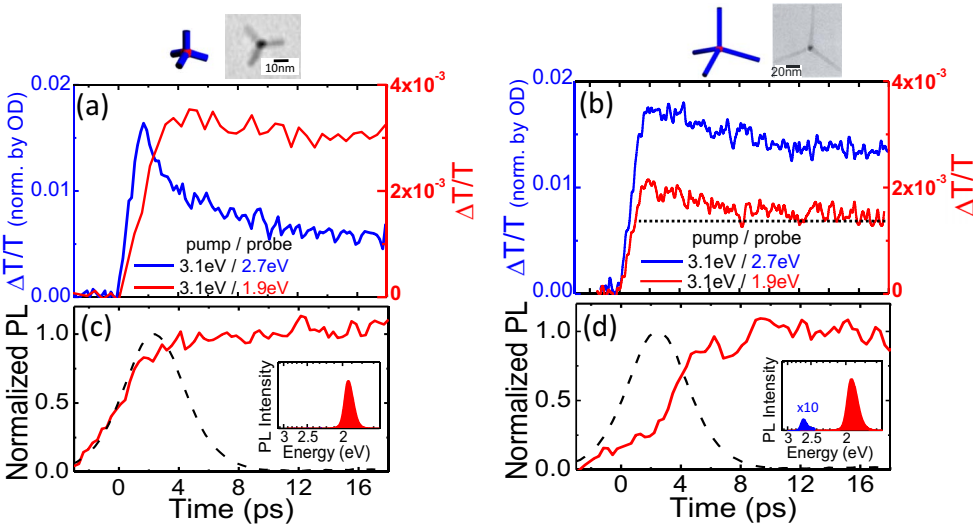

FIG. 2. (Color online) [(a) and (b)] Transient differential transmission and [(c) and (d)] photoluminescence decays for S1 (left column) and S2 (right column) at $T=5$ K. [(a) and (b)] Rise and decay of charge-carrier populations monitored by the normalized bleaching of CdS states (blue) and the bleaching of the CdSe core states (red). [(c) and (d)] Normalized PL emission transients measured at 1.9 eV (red) for S1 and S2, respectively. The dashed line in (c) and (d) shows the instrument response in time. The respective insets show the steady-state PL spectra. The weak CdS emission of S2 has been rescaled by a factor of ten.

heterostructures.[10] We remind here that single carriers can bleach only partially a specific transition while one electron-hole pair can result in complete bleaching because of the equal probability for the probe to experience absorption or stimulated emission.

The blue transient in Fig. 2(a) is representative for the population of the states calculated in Fig. 1(c), i.e., the band-edge transition in CdS. This bleaching sets on within 700 fs (carrier thermalization) and is followed by a fast decay (constant τ=2 ps) which corresponds to the rising part of the CdSe transient (red curve). The rise of CdSe is consistent with an increase in the population of core valence-band states [represented in Fig. 1(b)] and mainly reflects the relaxation of holes from the CdS into the CdSe core. The remaining CdS bleaching at long-time scales (16 ps) indicates the trapping of a few carriers in the arms. These time scales agree with recent pump-probe measurements on CdSe/CdS rods.[17] After the initial rise, completed within 4 ps, the CdSe bleaching decays on a long-time scale. It is important to compare these results with the time-resolved PL, which instead of being proportional to the sum of the occupation numbers, is proportional to the product, $\mathrm{PL}(\hbar\omega) \propto n_e(\hbar\omega)n_h(\hbar\omega)$. The PL signal, therefore, requires a non-negligible population of both electrons and holes in the emitting state. The rise in the PL of the CdSe core [Fig. 2(c)] follows the instrument response function (~5 ps) and reflects the presence of both charge carriers in the core within the time resolution (PL spectrum in the inset). This result is in accordance with the dynamics observed in the $\Delta T/T$ experiment, where the bleaching of the core reaches its maximum within 4 ps.

The sample S2 is expected to exhibit a more pronounced hole localization in the CdS arms (55 nm) with respect to S1, as a consequence of the relatively large distances for the hole to be captured into the core. Indeed, the blue $\Delta T/T$ transient in Fig. 2(b) signal, monitoring charge carriers in the CdS arms, does not show a fast depopulation as for S1 in Fig. 2(a). This indicates a longer residence time for carriers in CdS. Confirmation comes from the red transient in Fig. 2(b) probing the core, where the initial bleaching rise reaches the maximum at about half the value obtained for the S1 sample [cf. Fig. 2(a)]. Here, it is important to mention that the CdSe bleaching curves of the two samples were not normalized since the cores of the two tetrapod structures have the same size and therefore the same absorption cross sections. The observation that the maximum bleaching is not exactly the half of the one in S1, might be due to the small but not negligible probability for hole trapping in this sample. A further proof of the long residence time of one or both charge carriers in the CdS arms is given by the PL rise, shown in Fig. 2(d). In contrast to the resolution-limited rise of the S1 PL [Fig. 2(c)], a delayed rise is observed, and the maximum PL intensity is reached only at 12 ps for the S2 sample.

Both experiments, PL and $\Delta T/T$, monitoring the population of the core in S2 show that one carrier, namely, the hole, is initially missing [red curves in Figs. 2(b) and 2(d)]. This is demonstrated by the fact that since the PL signal is proportional to the product of carrier populations, the lack of hole population in the core in the first picoseconds after excitation is sufficient to delay the PL rise. This together with the experimental observation that half of the ΔT signal appears instantaneously in the core, show that mainly electrons are present in the core. Indeed according to our model calculations electrons relax immediately to the lowest state, bleaching the core transition [Fig. 1(c)]. This is valid for both samples. Therefore, by comparing the PL and $\Delta T/T$ transients of S2, we conclude that holes are not present in the core within the first picoseconds after excitation but instead become localized in trap states in the arms. If holes would be immediately present in the CdSe together with electrons, the $\Delta T/T$ signal of the S2 core would have the same amplitude as for S1 and the PL rise be within the 5 ps of the PL-setup resolution.

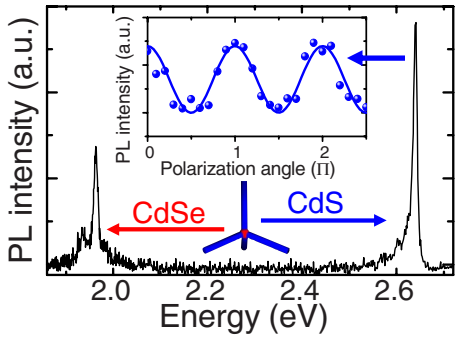

FIG. 3. (Color online) Low-temperature photoluminescence spectrum of a single S2 tetrapod showing emission from the CdSe (1.9 eV) and CdS (2.64 eV). The inset illustrates polarization anisotropy measured in emission recording the CdS PL as a function of the angle of rotation of a polarizer.

To confirm our hypothesis of a trap state localized in one of the CdS arms as shown in our model of Fig. 1(d), we performed PL spectroscopy on single S2 tetrapods as described in Refs. 12 and 18. Electron and hole localization, as shown in Fig. 1(d), should result in recombination and CdS PL. The steady-state PL spectrum of Fig. 3 shows two narrow features corresponding to the emission from CdS (2.63 eV) and CdSe (1.96 eV). This assignment is confirmed by the low-energy optical phonons, distinguished on the low-energy side of the peaks (CdSe=27.5 meV; CdS =38 meV).[19] Both transitions are observed on a single particle and provide evidence of electron-hole recombination in CdS. The inset of this figure shows the modulation of the CdS PL as a function of the angle of rotation of a polarizer placed in the detection path. The extracted polarization anisotropy P, defined as the ratio $(I_{\max}-I_{\min})/(I_{\max}+I_{\min})$, has a value of 0.9 and indicates that the emission originates from a single dipole.[12] We studied P for 20 single tetrapods, with all showing $P>0.7$ and thus indicating that both the electron and the hole are localized only in one of the four CdS arms.

We now comment on the initial decay of the electron population, seen in the $\Delta T/T$ of S2 [red curve in Fig. 2(b)], which is absent in S1. Here is important to note that the carrier population in the core of S2 is not increasing at later times, suggesting that the majority of holes trapped in the arm recombine with electrons and only a minor amount is detrapped and reaches the core. Effective radiative recombination in CdS as shown in Fig. 3 requires a wave-function overlap between the electron and the hole. Therefore, the

electrons initially localized in the core have to rearrange spatially, Fig. 1(d). This drag is expected to appear as a decrease in n_e of the core, i.e., a decay of ΔT. Indeed, the red $\Delta T/T$ transient in Fig. 2(b) shows an initial decay with a time constant of about 3 ps. Since the Coulomb drag effect should be on the order of our time resolution in the pump-probe experiment, it is conceivable that the 3 ps time constant for the decrease in the core $\Delta T/T$ corresponds to the hole trapping time. If holes were not localized in one of the tetrapod arms, the PL emission from the CdS would not be observable and the core bleaching signal should not show an initial decay of 3 ps.

In conclusion, we have presented experiments investigating the coupled real-space dynamics between electrons and holes in semiconductor nanocrystals with tetrapod shape. In short arm tetrapods, upon photoexcitation of carriers in the CdS arms, we observe a fast depopulation of CdS band-edge states. In tetrapods with longer CdS arms, the hole capture to the CdSe core is less probable and localization of the hole in one of the four CdS arms can occur. In this case the Coulomb potential of the hole drags the electron, initially centered in the core toward the arm, where they both localize and recombine resulting in emission from CdS.

Financial support by the Nanosystem Initiative Munich (NIM) of the DFG and the LMUexcellent program are acknowledged.

*Corresponding author; enrico.dacomo@physik.uni-muenchen.de

†Present address: Department of Physics and Materials Science, City University of Hong Kong, Hong Kong SAR.

[1] T. J. Gramila, J. P. Eisenstein, A. H. MacDonald, L. N. Pfeiffer, and K. W. West, Phys. Rev. Lett. **66**, 1216 (1991).

[2] U. Sivan, P. M. Solomon, and H. Shtrikman, Phys. Rev. Lett. **68**, 1196 (1992).

[3] A. Neukermans and G. S. Kino, Phys. Rev. B **7**, 2693 (1973).

[4] M. G. Bawendi, W. L. Wilson, L. Rothberg, P. J. Carroll, T. M. Jedju, M. L. Steigerwald, and L. E. Brus, Phys. Rev. Lett. **65**, 1623 (1990).

[5] A. Franceschetti and A. Zunger, Phys. Rev. Lett. **78**, 915 (1997).

[6] A. L. Efros, V. A. Kharchenko, and M. Rosen, Solid State Commun. **93**, 281 (1995).

[7] V. I. Klimov, J. Phys. Chem. B **104**, 6112 (2000).

[8] F. García-Santamaría, Y. Chen, J. Vela, R. D. Schaller, J. A. Hollingsworth and V. I. Klimov, Nano Lett. **9**, 3482 (2009).

[9] R. M. Kraus, P. G. Lagoudakis, A. L. Rogach, D. V. Talapin, H. Weller, J. M. Lupton, and J. Feldmann, Phys. Rev. Lett. **98**, 017401 (2007).

[10] A. Pandey and P. Guyot-Sionnest, J. Chem. Phys. **127**, 104710 (2007).

[11] D. V. Talapin *et al.*, Nano Lett. **7**, 2951 (2007).

[12] C. Mauser, T. Limmer, E. Da Como, K. Becker, A. L. Rogach, J. Feldmann, and D. V. Talapin, Phys. Rev. B **77**, 153303 (2008).

[13] J. Müller, J. M. Lupton, P. G. Lagoudakis, F. Schindler, R. Koeppe, A. L. Rogach, and J. Feldmann, Nano Lett. **5**, 2044 (2005).

[14] E. Hendry *et al.*, Phys. Rev. Lett. **96**, 057408 (2006).

[15] V. Klimov, P. H. Bolivar, and H. Kurz, Phys. Rev. B **53**, 1463 (1996).

[16] S. Logunov *et al.*, J. Phys. Chem. A **102**, 5652 (1998).

[17] M. G. Lupo *et al.*, Nano Lett. **8**, 4582 (2008).

[18] J. Müller, J. M. Lupton, A. L. Rogach, J. Feldmann, D. V. Talapin, and H. Weller, Phys. Rev. Lett. **93**, 167402 (2004).

[19] Landolt Börnstein, *II-VI and I-VII Compounds; Semimagnetic Compounds* (Springer-Verlag, Berlin, 1999), Vol. 41B.